

## THERMAL AND OPTICAL CHARACTERIZATION OF TETRATHYLENE GLYCOL – BASED SOLAR NANOFLUID AT HIGH TEMPERATURE CONDITIONS

Gimeno-Furio A, Navarrete N, Martinez-Cuenca R, Mondragon R, Julia J. E.\* and Hernandez L

\*Author for correspondence

Departamento de Ingenieria Mecanica y Construccion.

Universitat Jaume I,

12071 Castellon de la Plana,

España,

E-mail: enrique.julia@uji.es

### ABSTRACT

Nanofluids are defined as dilute suspensions with solid particles smaller than 100 nm. Nanofluids present some important advantages over the conventional colloidal suspensions such as high stability, reduced particle clogging and high heat transfer capabilities. Most of published works have been focused on the increment of thermal conductivity in water-based nanofluids with high nanoparticle loads.

Solar nanofluids are a type of nanofluids with low nanoparticle loads and suitable for direct solar radiation harvesting. In this case, nanoparticles in the heat transfer fluid directly absorb the solar radiation, transferring the heat to the heat transfer fluid. In this way, high efficiency from solar radiation to thermal energy can be obtained since the heat exchange area (nanoparticle surface area) is extremely high and the peak temperature is inside the heat transfer fluid. In most published works, thermal and optical characterizations of solar nanofluids are performed at room temperature conditions, far away from experimental conditions found in real applications.

In this work, a complete thermal and optical characterization of a tetraethylene glycol – based nanofluid using tin nanoparticles have been performed. Nanoparticle morphology and nanoparticle cluster size have been characterized at room conditions and thermal conductivity, specific heat capacity and transmission spectrum have been measured at different temperatures between 50°C and 150°C. Nanoparticle morphology has been characterized by Transmission Electron Microscope and cluster size by Dynamic Light Scattering technique, thermal conductivity have been measured by the hot wire technique, the specific heat capacity by a Differential Scanning Calorimeter and the transmission spectrum by a fiber optic based spectrometer and a special designed nanofluid cuvette with controlled temperature conditions.

### INTRODUCTION

Nanofluids are defined as heat transfer and/or thermal energy storage fluids with enhanced heat transfer properties by the addition of nanoparticles. In 1993, Masuda et al. [1] used nanoparticles for the enhancement of the thermal conductivity of a fluid. Two years later, S.U.S. Choi [2] coined the term nanofluid and defined it as a dilute-stable suspension of particles with sizes below 100 nm. These suspensions present

higher specific surface than conventional colloidal suspensions and are more stable than conventional slurries. In this way, nanofluids allow to some extent, to introduce appreciable amounts of solids into liquids, preserving the transport properties of the liquid at the same time. Thus, solid advantages can be incorporated into liquid using standard pumping equipment. First nanofluid publications were focused on the thermal conductivity increment using water as base fluid. In the last years, nanofluids based on higher temperature heat transfer and/or thermal storage fluids have gained attention. A complete reference of recent works can be found in [3-5].

Stability is one of the key issues of nanofluids. Nanoparticles collisions are inevitable due to its continuous movement inside the liquid produced by the Brownian motion. If nanoparticle agglomeration is not avoided, nanoparticle cluster size increases and sedimentation occurs. Nanoparticle agglomeration can be avoided by adjusting the pH in water-based nanofluids. If the pH value is far away from the isoelectric point, nanoparticles surface will be electrically charged and they will repulse each other. In the case of nanofluids based on organic liquids, nanoparticles surface should be functionalized with appropriate organic molecules in order to prevent agglomeration.

In most of nanofluid published works, an increment in thermal conductivity is obtained. However, an important increment of viscosity is also found, reducing the potential applications of nanofluids. In order to overcome this situation, efforts in reducing nanofluid viscosity are in progress [6] and additional advantages of solids have been explored.

In 2009, solar nanofluids were proposed as volumetric solar radiation receivers [7-8]. In this type of nanofluids, transparent heat transfer fluids in the visible and near infrared range (such as water, glycols, thermal oils and molten salts) are used and nanoparticles showing a high radiation absorption spectrum in this wavelength range absorb the solar radiation. Thus, the solar radiation absorption is performed by the nanoparticles in a volumetric (3D) way, using a relative large thickness of the nanofluid (in contrast with the conventional solar receivers, where the solar radiation absorption is produced in 2D using black surfaces). Depending on the nanoparticle type, solar absorption can cover almost the whole solar spectrum (carbon and metal oxide nanoparticles) or only selected wavelengths (gold and silver nanoparticles). Although solar nanofluids have

been proposed for high temperature applications, most of its thermal and optical properties have not been measured at their process operating conditions

Glycols have been used as base fluid of nanofluids since they can work at high temperature conditions and the increment in viscosity due to nanoparticle addition is low [9, 10]. Furthermore, metal oxide nanoparticles have been used in solar nanofluids since they have a quite flat absorption spectrum in the visible and infrared ranges [7]. An additional advantage of metal oxides is its easy stabilization in glycols without the use of stabilizers [9, 10].

## NOMENCLATURE

$Ab$	[-]	Absorption
$C_p$	[J / g K]	Specific Heat
$d$	[nm]	Primary diameter
$D$	[nm]	Cluster equivalent diameter
$k$	[W/m K]	Thermal conductivity
$T$	[-]	Transmission
$V$	[m <sup>3</sup> ]	Volume

### Special characters

$\alpha$	[-]	Particle size parameter
$\phi$	[-]	Volumetric concentration
$\lambda$	[nm]	Wavelength
$\rho$	[kg /m <sup>3</sup> ]	Density

### Subscripts

$bf$	Base fluid
$nf$	Nanofluid
$p$	Particle
$v$	Volumetric

### Abbreviations

$DSC$	Differential Scanning Calorimeter
$DLS$	Dynamic Light Scattering
$NF$	Nanofluid
$Sn$	Tin
$TEG$	Tetraethylen glycol
$TEM$	Transmission Electronic Microscope
$wt$	Weight concentration

## MATERIALS AND METHODS

### Nanofluid preparation

Nanofluid is prepared by the two-step method. In this method the nanoparticles are produced by chemical or physical procedures and, later, dispersed in the base fluid and additives (if any). Tetraethylen glycol (TEG, Sigma Aldrich, 99.99%) and tin nanoparticles (Sn, US Nano,  $d_p < 80$  nm) are used as purchased. The base fluid and nanoparticles were weighted in an analytical balance (Kern ABS,  $\pm 0.001$  mg) and sonicated with a high power ultrasound probe for 5 minutes (Sonopuls HD2200, Bandelin) in ice bath.

### Nanoparticle morphology and nanoparticle cluster size

Size and shape of primary nanoparticles were observed by means of Transmission Electron Microscopy (TEM, JEOL 2100) operating at a voltage of 100kV.

The size distributions of nanoparticles in suspension were measured by dynamic light scattering (DLS, Zetasizer nano ZS, Malvern Instruments) with a 173° scattering angle. Particle size was measured from the velocity of the particles due to their Brownian motion by means of the Einstein-Stokes equation. Nanoparticle diameter measurement range is 0.3 nm – 10  $\mu$ m with an uncertainty of  $\pm 2\%$ . DLS measurements were performed at room temperature.

### Transmission spectrum

Transmission spectrum is measured by an optical fiber spectrometer (StellarNet, model GREEN WAVE) with a wavelength range from 350 nm to 1150 nm wavelength and a spectral resolution of 0.5 nm.

A solar simulator (ORIEL model 66475-150XF-R22) is used as light source. The light produced by the Xenon lamp of the simulator is reflected in a 45° mirror, passes through a high temperature cuvette, and then the light is collected by a lens next into the spectrometer. In this way, light source and spectrometer are not in direct contact with the nanofluid sample and high temperature measurements are possible.

The high temperature cuvette has 10 mm beam path length and it is composed of a metal tube with two quartz windows and a heater. There are also two thermocouples to control the fluid temperature: one of them is inside the cuvette in contact with the nanofluid and the other one is in the cuvette case to control the heater temperature. An outline assembly is shown in Figure 1.

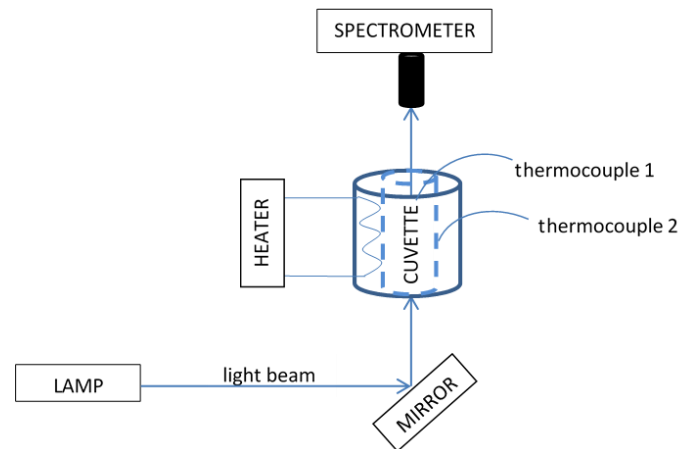


**Figure 1** Transmission spectrum setup

The measurement procedure is as follows. First, a spectrum is obtained without fluid and the lamp switch off (dark). Then, the lamp is switch on and a new transmission spectrum is measured (reference). Finally, the cuvette is filled with the liquid, set to the measurement temperature and, after 20 minutes of stabilization, a new transmission spectrum is obtained (sample). Finally, the transmittance spectrum can be obtained using equation (1):

$$T(\%) = \frac{(sample - dark)}{(reference - dark)} 100 \quad (1)$$

The absorption spectrum can be obtained as  $A_b(\%) = (100 - T(\%))$  if reflection and scattering losses are neglected. In this work, reflection losses are taken into account in the reference spectrum measurement. Scattering losses can be considered small if the particle size parameter,  $\alpha$ , and the particle volumetric fraction,  $\phi$ , are below 10 and 0.01, respectively.  $\alpha$  and  $\phi$  depend on the nanofluid and are defined in equations (2) and (3), respectively.

$$\alpha = \pi d_p / \lambda \quad (2)$$

$$f = V_p / V \quad (3)$$

where  $d_p$  is the primary diameter of the particles,  $\lambda$  the wavelength,  $V_p$  the volume occupied by the nanoparticles and  $V$  the total volume of the sample. In this work,  $\alpha$  and  $\phi$  values are below 10 and 0.01, respectively. Consequently,  $A_b$  can be directly obtained from the transmission spectrum.

### Thermal conductivity

The thermal conductivity of all nanofluids was measured using a KD2 Pro conductimeter (Decagon Devices Inc.) based on the Transient Hot Wire technique. The sample was introduced in a sealed glass tube (22 ml) where the sensor was inserted vertically.

To carry out the test at high temperature conditions, the tube is submerged in a thermostatic bath where the temperature is controlled. The reading time was set at 1 minute to minimize the temperature difference between the fluid and the needle, being the maximum difference obtained of 0.3 degrees. A period of time of 1 hour was waited for the sample to reach the desired temperature before any test. After that time, 6 measurements were done for each nanofluid sample. Within this time the bath was switched off. It was important to wait for about fifteen minutes between readings to recover the temperature after the heat pulse applied to the nanofluid.

### Specific Heat

The specific heat,  $C_p$ , was measured in a Differential Scanning Calorimeter (DSC), model DSC2 (Mettler Toledo, USA). The calculation of the specific heat capacity is based on the DIN standard (DIN 51007). The specific heat is calculated from the mass of the sample and the heat flux needed for the heating and cooling dynamic segments. In order to avoid liquid evaporation, the DSC crucible (Aluminium) was sealed.

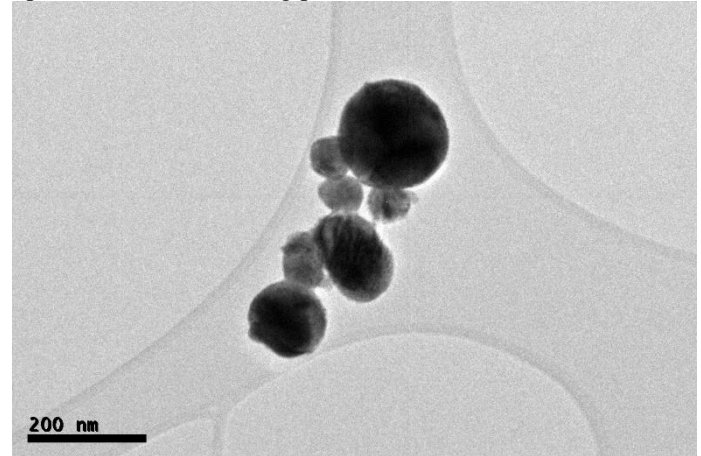
The sequence used in the determination was as follows: isotherm of 5 minutes at 50°C, dynamic segment from 50°C to 150°C at heating rate of 10°C/min and isotherm of 5 minutes at 150°C and dynamic segment from 150°C to 50°C at cooling rate of 10°C/min.

## RESULTS

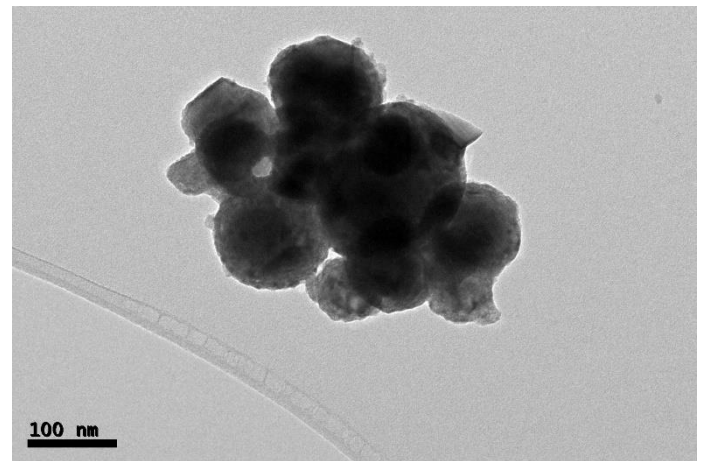
### Nanoparticle morphology and nanoparticle cluster size

Figure 2 shows TEM images of Sn nanoparticles. It is possible to observe that nanoparticles have spherical shape and a wide range of diameters. In some cases, nanoparticle clusters

can be found. In addition, metal oxide can be observed in the nanoparticle surface, showing partial oxidation.

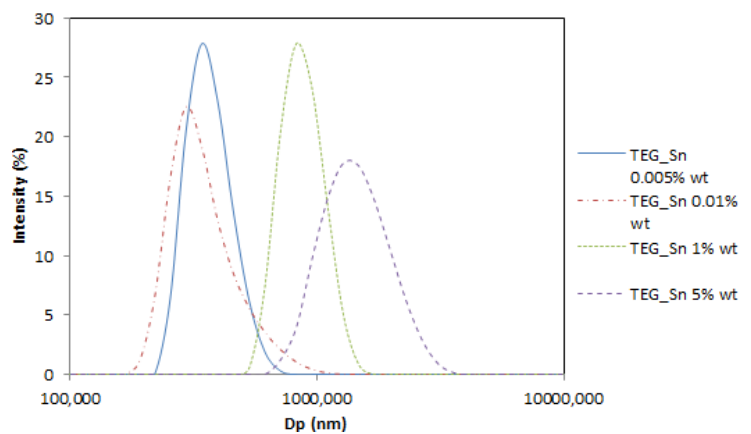


a)



b)

Figure 2 TEM images of Sn nanoparticles



a)

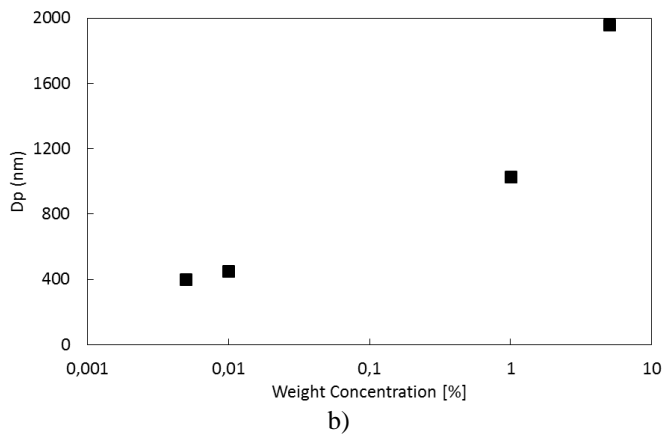


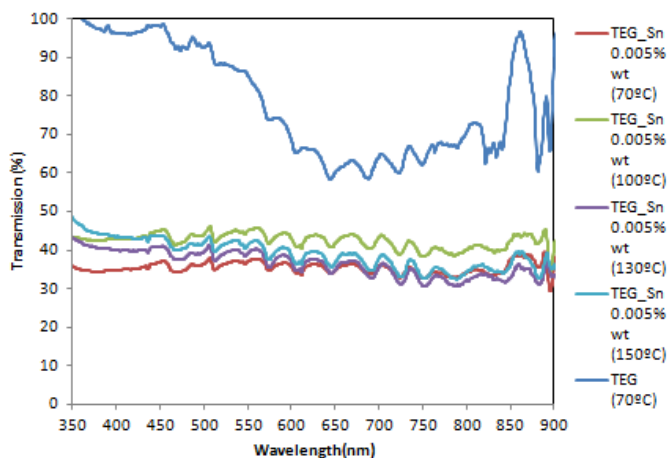
**Figure 3** DLS measurements of nanoparticle cluster size at different nanoparticle concentrations, a) cluster size distribution; b) average values

It is possible to observe that cluster size presents a wide distribution for all nanoparticle concentrations and that the width increases with nanoparticle concentration. In addition, cluster average size is higher than the nanoparticle primary diameter, even for very low nanoparticle concentrations. This result confirms previous TEM images (Figure 2) in which nanoparticle are in an aggregated state that can not be broken by the ultrasound probe. The high dependence of the nanoparticle cluster size with nanoparticle concentration is also stated by previous authors [11, 12].

**Transmission spectrum**

Figures 4 and 5 show transmission spectrum for TEG and Sn TEG-based nanofluids. Only results from 350 nm to 900 nm are shown since the mirror used in the experimental setup cuts higher wavelengths.

**Figure 4** Transmission spectrums of TEG and Sn TEG-



based nanofluids for nanoparticle concentration of 0.005% wt. and different temperatures

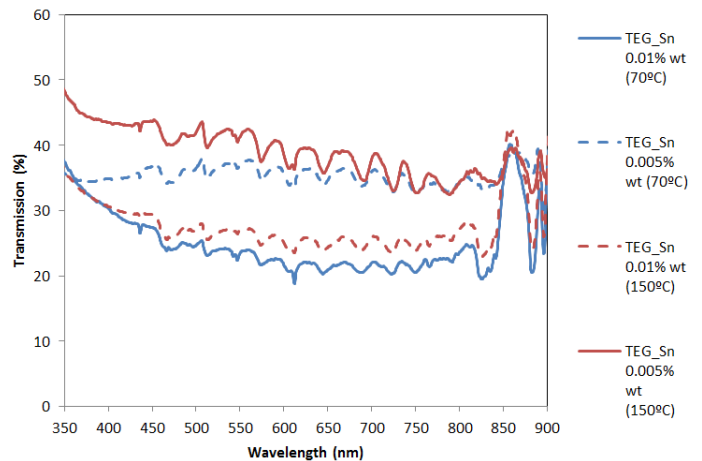


**Figure 5** Transmission spectrums of Sn TEG-based nanofluids for nanoparticle concentration of 0.005% wt. and 0.01% wt. and different temperatures

TEG presents high transmission values for all wavelengths, especially from 380 nm to 530 nm. This wavelength range match with the maximum of the solar irradiance (Figure 6). Consequently, TEG can not be directly used for direct absorption of solar radiation. The addition of Sn nanoparticles allows absorbing the solar radiation in all the solar wavelength range. In addition, results show that the absorption of the Sn TEG-based nanofluid is not dependant on the wavelength or the nanofluid temperature. Also, transmission values are linear with nanoparticle concentration. This fact makes Sn TEG-based nanofluid suitable as solar nanofluid in high temperature conditions.

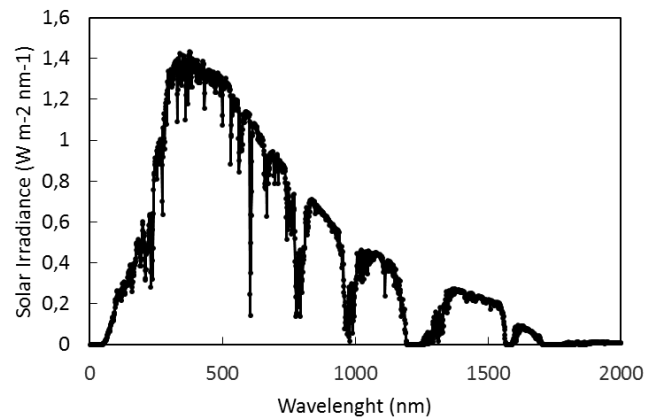


**Figure 6** Solar spectrum ASTM G173 [13]

**Thermal conductivity**

Figures 7 and 8 present thermal conductivity measurements of TEG and Sn TEG-based nanofluids at different temperatures and nanoparticle concentrations. Only 1% wt. and 5% wt. nanoparticle concentrations are shown since for lower concentration, any increment was observed.

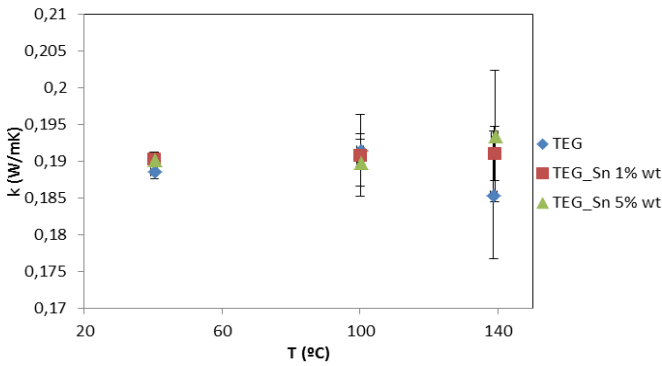


Figure 7 Thermal conductivity results

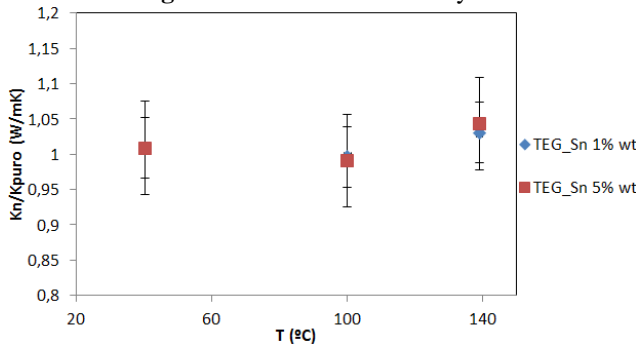


Figure 8 Increment in thermal conductivity for different nanoparticle concentrations and sample temperatures

It is possible to observe that only for 5% wt. an appreciable increase in  $k$  is observed, which also grows as the temperature rises. These results are in agreement with previous results at lower temperature conditions [12] and with standard correlations used to predict the thermal conductivity in nanofluids [14]

$$k_{nf} = \frac{k_p + 2k_{bf} + 2(k_p - k_{bf})\phi}{k_p 2k_{bf} - 2(k_p - k_{bf})\phi} k_{bf} \quad (4)$$

where  $\phi$  is the volumetric concentration of nanoparticles and  $p$ ,  $nf$  and  $bf$  subscripts denote particle, nanofluid and base fluid, respectively.

### Specific heat

Figure 9 shows specific heat measurements of TEG and Sn TEG-based for 1% wt. and 5% wt. nanoparticle concentrations. It is possible to observe that similar  $C_p$  values can be found for heating and cooling measurements. TEG specific heat values are in agreement with the data given by the supplier. TEG-based nanofluids present lower  $C_p$  values than TEG since solid  $C_p$  is low (in the case of Sn,  $C_p = 0.21$  J/g K). Results found are in accordance with the mixing rule,

$$C_{p,nf} = \frac{(1-\phi)\rho_{bf}C_{p,bf} + \phi\rho_p C_{p,p}}{(1-\phi)\rho_{bf} + \phi\rho_p} \quad (5)$$

where  $\rho$  is the density.

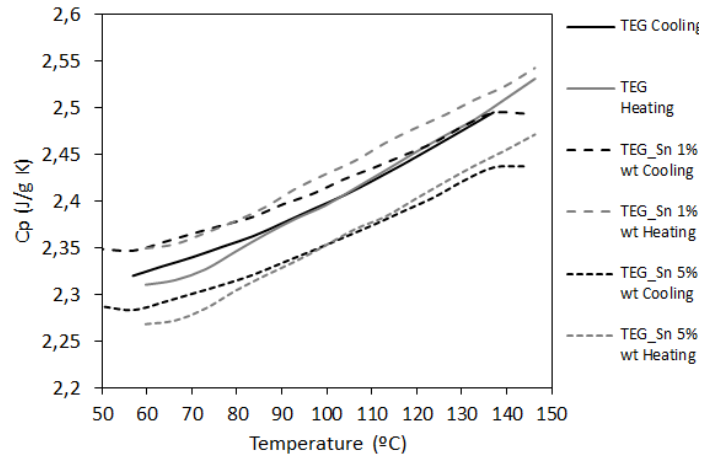


Figure 9 Specific heat measurements

## CONCLUSION

Sn TEG-based nanofluids have been synthesized and characterized at high temperature conditions. This type of nanofluid can be used for solar harvesting applications since it has a constant absorption spectrum in all the solar radiation wavelength even for high temperature conditions. Thermal properties of Sn TEG-based nanofluids have been characterized at high temperature conditions showing expected results.

## REFERENCES

- [1] Masuda H., Ebata A., Teramae K., Hishinuma N., Alteration of thermal conductivity and viscosity of liquid by dispersing ultrafine particles (dispersion of gamma-al<sub>2</sub>o<sub>3</sub>, sio<sub>2</sub> and tio<sub>2</sub> ultrafine particles), *Netsu Bussei* 4, 1993, pp. 227–233.
- [2] Choi S.U.S., Enhancing thermal conductivity of fluids with nanoparticles. *ASME Int. Mech. Eng. Congress and Exp.*, San Francisco, CA, USA. doi:10.1115/1.2825978. 1995.
- [3] Wang X.- Q., Mujumdar A.S., Heat transfer characteristics of nanofluids: a review, *Int. J. Therm. Sci.* 46, 2007, pp. 1–19, doi:10.1016/j.ijthermalsci.2006.06.010.
- [4] Ozerinç S., Kakaç S., Yazicioglu A. G., Enhanced thermal conductivity of nanofluids: a state-of-the-art review, *Microfluid. Nanofluid.* 8, 2010, pp. 145–170. doi:10.1007/s10404-009-0524-4.
- [5] Taylor R. A., Coulombe S., Otanicar T., Phelan P., Gunawan A., Wei Lv, Rosengarten G., Prasher R., Tyagi H., Small particles, big impacts: A review of the diverse applications of nanofluids *J. Appl. Phys.* 113, 2013. 011301.
- [6] Zyla G., Cholewa M., On unexpected behavior of viscosity of diethylene glycol-based MgAl<sub>2</sub>O<sub>4</sub> nanofluids. *RSC Adv.*, 4, 2014, 26057
- [7] Taylor R. A., Phelan P. E., Adrian R. J., Prasher R. S., Experimental results for light-induced boiling in water-based graphite nanoparticle suspensions, in *Proceedings of the ASME 2009 Summer Heat Transfer Conference* 2009, pp. 1–9.
- [8] Taylor R. A., Phelan P. E., Otanicar T. P., Walker C. A., Nguyen M., Trimble S., Prasher R. S. Applicability of nanofluids in high flux solar collectors *J. Renewable Sustainable Energy* 3, 2011, 023104. <http://dx.doi.org/10.1063/1.3571565>

- [9] Pastoriza-Gallego M. J., Lugo L., Legido J. L., Piñeiro M. M. Rheological non-Newtonian behaviour of ethylene glycol-based Fe<sub>2</sub>O<sub>3</sub> nanofluids. *Nanoscale Res Lett*. 6 2011; 560.
- [10] Cabaleiro D., Pastoriza-Gallego M. J., Gracia-Fernandez C., Piñeiro M. M., Lugo L., Rheological and volumetric properties of TiO<sub>2</sub>-ethylene glycol nanofluids. *Nanoscale Res Lett*. 13, 2013, 286.
- [11] Mondragon R., Segarra C., Martínez-Cuenca R., Julia J. E., Jarque J. C., Experimental characterization and modeling of thermophysical properties of nanofluids at high temperature conditions for heat transfer applications. *Powder Technology* 249, 2013, pp. 516–529.
- [12] Alberola J. A., Mondragon R., Julia J. E., Hernandez L., Cabedo L. Characterization of halloysite-water nanofluid for heat transfer applications. *Applied Clay Science* 99, 2014, pp. 54–61.
- [13] Standard Tables for Reference Solar Spectral Irradiance: Direct Normal and Hemispherical on 37° Tilted Surface. ASTM G173-03(2012).
- [14] Maxwell J. C., A Treatise on Electricity and Magnetism, Clarendon Press, Oxford, UK, 1873.